Advance Publication Cover Page

Bulletin of the Chemical Society of Japan

Identification of Intermediates in Peroxidase Catalytic Cycle of a DNAzyme Possessing Heme

Ryosuke Shinomiya, Haruka Araki, Atsuya Momotake, Hiroaki Kotani,
Takahiko Kojima, and Yasuhiko Yamamoto*

Advance Publication on the web July 13, 2019

doi:10.1246/bcsj.20190157

Identification of Intermediates in Peroxidase Catalytic Cycle of a DNAzyme Possessing Heme

Ryosuke Shinomiya,[1] Haruka Araki,[1] Atsuya Momotake,[1] Hiroaki Kotani,[1] Takahiko Kojima,[1] and Yasuhiko Yamamoto*[1,2,3]

[1]Department of Chemistry, University of Tsukuba, Tsukuba 305-8571

[2] Tsukuba Research Center for Energy Materials Science (TREMS), University of Tsukuba, Tsukuba 305-8571

[3] Life Science Center for Survival Dynamics, Tsukuba Advanced Research Alliance (TARA), University of Tsukuba, Tsukuba 305-8577

E-mail:yamamoto@chem.tsukuba.ac.jp

Yasuhiko Yamamoto
Dr. Yasuhiko Yamamoto received his Ph. D. in Chemistry from University of California, Davis, in 1986.
He is currently Professor of Chemistry at University of Tsukuba.
His research interests are primarily in the arears of bioinorganic chemistry and NMR spectroscopy.

Abstract

Heme in the ferric state (heme(Fe^{3+})) binds to G-quadruplex DNAs to form stable complexes that exhibit enhanced peroxidase activities. The complexes are considered as DNAzymes possessing heme as a prosthetic group (heme-DNAzymes), and have been extensively investigated as promising catalysts for a variety of applications. On ESR and stopped-flow measurements, an iron(IV)oxo porphyrin π-cation radical known as Compound I was detected in reaction mixtures of heme-DNAzymes and hydrogen peroxide. This finding not only resolved the long-standing issue of the mechanism underlying the enhancement of the peroxidase activity of heme(Fe^{3+}) in the scaffold of a G-quadruplex DNA, but also provided new insights as to the design of novel heme-DNAzymes.

Keywords: DNA enzyme, Heme, Peroxidase activity.

1. Introduction

Heme, i.e., an iron-protoporphyrin IX complex (Figure 1A), in the ferric state (heme(Fe^{3+})) binds to G-quadruplex DNAs to form stable complexes that exhibit enhanced peroxidase activities.[1-5] These complexes are considered as DNAzymes possessing heme (heme-DNAzyme) as a cofactor, and have been extensively investigated as promising catalysts for a variety of applications. Despite the exponential increase in the number of papers on heme-DNAzyme applications published in recent years,[6-21] their structure-function relationship has largely remained unknown.[4,22-24] A G-quadruplex DNA is stabilized by a unique structural motif, known as the G-quartet, which is formed through a cyclic and coplanar association of four guanine bases through Hoogsteen hydrogen bonds (Figure 1B).[25] We demonstrated that heme(Fe^{3+}) (or heme(Fe^{2+})) binds selectively to the 3'-terminal G-quartet (G6 G-quartet) of an all parallel-stranded tetrameric G-quadruplex DNA formed from a single repeat sequence of the human telomere, $(d(TTAGGG))_4$ (6mer), to form a complex (heme(Fe^{3+})-6mer or heme(Fe^{2+})-6mer complex) (Figure 1C).[26-32] The heme(Fe^{3+})-6mer complex has been reported to exhibit peroxidase activity[32] as well as various

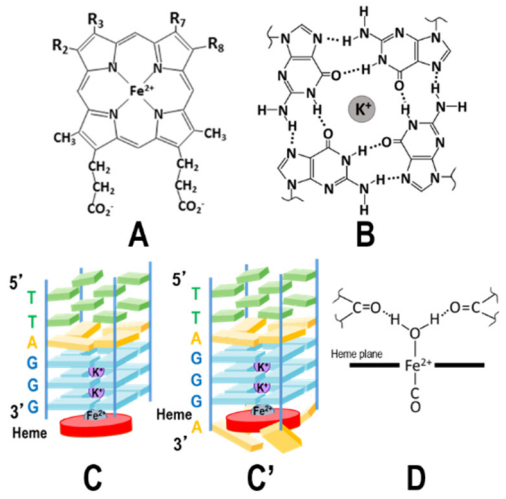

Figure 1. Structures and numbering schemes for heme(Fe^{2+}) (A), Molecular structure of the G-quartet (B), and schematic representation of complexes between heme(Fe^{2+}) and all parallel-stranded tetrameric G-quadruplex DNAs of d(TTAGGG) and d(TTAGGGA), (C) and (C'), respectively, and the heme(Fe^{2+}) coordination structure of a carbon monoxide (CO) adduct of the complex (D). In the complexes, CO binds to the heme Fe atom on the side of the heme opposite to the G6 G-quartet, and then a water molecule (H_2O), sandwiched between the heme and G6 G-quartet planes, is coordinated to the Fe atom as another axial ligand, *trans* to the CO ligand.

spectroscopic properties remarkably similar to those of the oxygen storage hemoprotein myoglobin[26-28, 30, 31] (Mb). Hence the heme(Fe^{3+})-6mer complex could be considered as an excellent model for elucidating the structure-function relationships in heme-DNAzymes.

It is often assumed that the peroxidase activity of a heme-DNAzyme is elicited through a reaction mechanism similar to that of peroxidases such as horseradish peroxidase (HRP) (Scheme 1A). The assumption is not indisputable, because

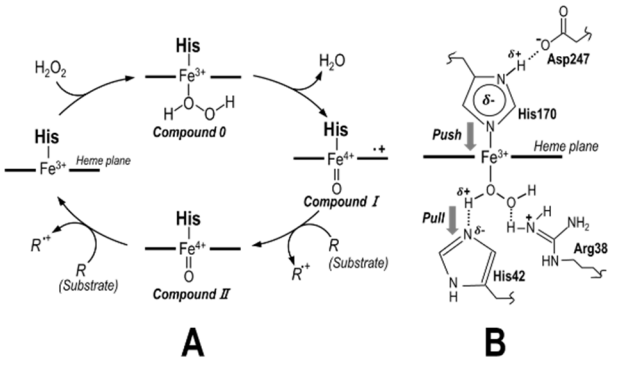

Scheme 1. Catalytic cycle of horseradish peroxidase (HRP)[43] (A) and schematic representation of the active site of HRP[44] (B). In (B), amino acid residues involved in the "push-pull mechanism"[33, 42] are shown.

functional groups involved in the catalytic cycle of a heme-DNAzyme ought to be different from those of HRP. The catalytic cycle of HRP as well as of cytochrome P450 proceeds through the iron(IV)oxo porphyrin π-cation radical intermediate known as Compound I formed through heterolytic O-O bond cleavage of Fe-bound hydrogen peroxide (H_2O_2), and this process is controlled through the so-called "push-pull" mechanism (Scheme 1B).[33-44] The "push" effect in HRP is provided by the electron-donating effect of the proximal histidine (His170), which possibly contributes to stabilization of higher oxidation states of the heme Fe atom during the catalysis.[33-37] On the other hand, during the catalytic cycle of HRP, the distal His (His42) accepts a proton from the proximal oxygen atom of Fe-bound H_2O_2 and transfers it to the distal oxygen one to generate leaving H_2O. Furthermore, in concert with the action of His42, a nearby cationic amino acid side chain (Arg38) facilitates heterolytic O-O bond cleavage through stabilization of the developing negative charge on the distal oxygen atom during the bond cleavage (Scheme 1B). Thus, the "pull" mechanism is provided by the combination of His42 and Arg38.[38-42]

We found, through characterization of the peroxidase activities of complexes possessing a series of chemically-modified hemes, that the complex monotonously increases with increasing electron density of the heme Fe atom, supporting the "push" mechanism in the catalytic cycle of the complex.[32] Furthermore, the "pull" mechanism in the catalytic cycle of the complex was also confirmed by comparative studies on complexes of heme(Fe^{3+}) with all parallel-stranded monomeric G-quadruplex DNAs formed from inosine(I)-containing sequences, i.e., d(TAGGGTGGGTTGGGTGIG) DNA(18mer) and d(TAGGGTGGGTTGGGTGIGA) DNA(18mer/A).[45] We found that heme(Fe^{3+}) binds to the 3'-terminal G-quartet of the G-quadruplex DNAs to form complexes exhibiting peroxidase activities, and that the activity of the heme(Fe^{3+})-DNA(18mer/A) complex was greater than that of the heme(Fe^{3+})-DNA(18mer) one, indicating that the 3'-terminal A, i.e., A19, of the sequence acts as a general acid-base catalyst that promotes the catalytic reaction of the heme(Fe^{3+})-DNA(18mer/A) complex.

In this study, we attempted to capture short-lived intermediates in the peroxidase catalytic cycle of the heme(Fe^{3+})-6mer complex and a related complex composed of heme(Fe^{3+}) and all parallel-stranded tetrameric G-quadruplexes, $(d(TTAGGGA))_4$, (6mer/A), and (heme(Fe^{3+})-6mer/A complex) through ESR spectroscopy and stopped-flow experiments. We could detect a convex peak at $g = \sim 2$ in the ESR spectra of frozen mixtures of the complexes and H_2O_2, which is characteristic of Compound I.[46, 47] The UV-vis absorption signatures of Compound I[48, 49] could also be detected in the spectrum of a mixture of heme(Fe^{3+})-6mer/A complex and H_2O_2, recorded through stopped-flow experiments. These results clearly demonstrated generation of Compound I in the catalytic cycle of the heme-DNAzyme. This finding provides the fundamental basis of the structure-function relationship in heme-DNAzymes.

2. Experimental

Heme-DNA Complex Preparation. DNA sequences, d(TTAGGG) and d(TTAGGGA), purified with a C-18 Sep-Pak cartridge, were purchased from Tsukuba Oligo Service Co. The oligonucleotides were obtained by ethanol precipitation and then desalted with Microcon YM-3 (Millipore, Bedford, MA). The concentration of each oligonucleotide was determined spectrophotometrically using the absorbance at 260 nm (molar extinction coefficients $\lambda_{260} = 6.89 \times 10^4$ and 8.43×10^4 $cm^{-1}M^{-1}$ for d(TTAGGG) and d(TTAGGGA), respectively). Heme(Fe^{3+}) was purchased from Sigma-Aldrich Co. Preparation of the heme(Fe^{3+})-DNA complexes was carried out by mixing 5 - 20 μM heme(Fe^{3+}) and 10 - 40 μM DNA as described previously.[31]

Measurement of UV-Vis Absorption and Amplex Red Oxidation Kinetics. UV-Vis absorption spectra were recorded at 298 K with a Beckman DU 640 spectrophotometer using 50 mM potassium phosphate buffer, pH 6.80, containing 300 mM KCl as the solvent. Horseradish peroxidase (HRP) was purchased as a lyophilized powder from Sigma-Aldrich Co. and used without further purification. The chromogenic substrate, Amplex Red (10-acethyl-3,7-dihydroxyphenoxazine), was purchased from Sigma-Aldrich, and the reaction was monitored by following the appearance of the oxidized product, 7-hydroxyphenoxazin-3-one (Resorufin) through the following reaction, which absorbs light at ~570 nm.[32]

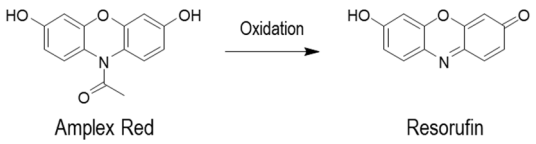

Kinetic studies were performed on a Beckman DU640 spectrometer. $(d(TTAGGG))_4$ and $(d(TTAGGGA))_4$ in 50 mM potassium phosphate buffer, pH 6.80, were heat-denatured at 363 K for 5 min., followed by cooling to 298 K. Amplex Red was dissolved in dimethylformamide to prepare a 10 mM stock solution. Heme(Fe^{3+}) and then Amplex Red were added to 0.1 μM and 50 μM, respectively, to 10 μM DNA in 50 mM potassium phosphate buffer, pH 6.80. To initiate the oxidation reactions, 5 – 200 mM hydrogen peroxide (H_2O_2) were added to the solution mixture. For the kinetic measurements of the HRP system, 1 – 100 μM H_2O_2 was added to the solution mixture of 0.01 μM protein and 50 μM Amplex Red in 50 mM potassium phosphate buffer, pH 6.80, to initiate the reactions. The initial slope (R_0) of the time evolution of 570-nm absorbance due to Resorufin was used as an index for the peroxidase activities of the complexes and HRP.

Electron Spin Resonance (ESR) Spectroscopy. ESR spectra were recorded on a Bruker BioSpin X-band spectrometer (EMXPlus9.5/2.7) with a liquid helium transfer system under non-saturating microwave power conditions (4.0 mW) operating at 9.394 GHz. The magnitude of the modulation was chosen to optimize the resolution and the signal-to-noise (S/N) ratio of the

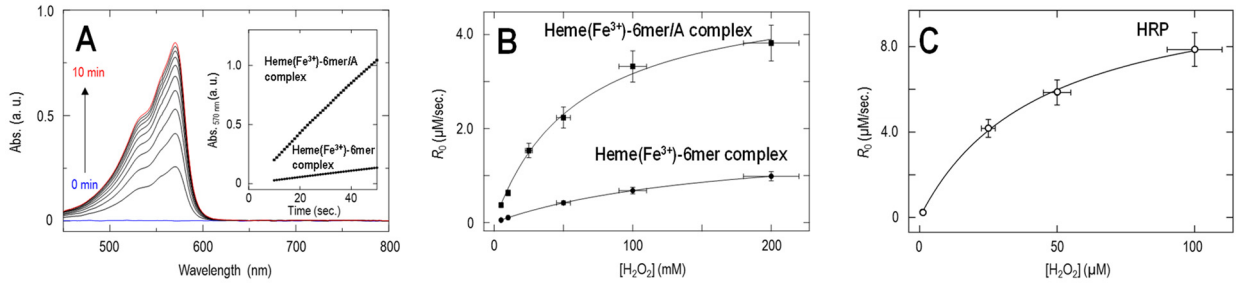

Figure 2. The time evolution of the oxidation reaction of Amplex Red (10-acethyl-3,7-dihydroxyphenoxazine) with the heme(Fe^{3+})-6mer/A complex and H_2O_2, monitored by following the appearance of the oxidized product, 7-hydroxyphenoxazin-3-one (Resorufin) (A). Time-evolution of 570-nm absorbance due to Resorufin produced on the reactions of the heme(Fe^{3+})-6mer and heme(Fe^{3+})-6mer/A complexes is shown in the inset. Samples comprised 1.0 μM heme(Fe^{3+}), 10 μM DNA, 50 μM Amplex Red, and 5 mM H_2O_2 in 50 mM potassium phosphate buffer, pH 6.80, at 298 K. The values of 0.05 ± 0.01 and 0.37 ± 0.04 μM/s were obtained from the initial slopes (R_0) for the heme(Fe^{3+})-6mer and heme(Fe^{3+})-6mer/A complexes, respectively. Plots of the R_0s for the heme(Fe^{3+})-6mer and heme(Fe^{3+})-6mer/A complexes (B), and HRP (C), as a reference, against the concentration of H_2O_2 ([H_2O_2]). The HRP sample comprised 0.05 μM protein, 50 μM Amplex Red, and 1-100 μM H_2O_2 in 50 mM potassium phosphate buffer, pH 6.80, at 298 K.

observed spectrum (modulation amplitude, 5−20 G; modulation frequency, 100 kHz).

For ESR samples of heme-DNA complexes, 0.1 mM heme and 0.1 mM DNA were mixed in 50 mM potassium phosphate buffer, pH 6.80, and 300 mM KCl, and then 15 mM H_2O_2 was added. The mixed solution was immediately frozen for the measurement at 5 K under a He atmosphere.

Stopped-Flow Experiments. Formation of Compound I was monitored by stopped-flow experiments performed on a UNISOKU USP-SFM-CRD10 stopped-flow spectrometer equipped with a multichannel photodiode array, a 150-W xenon lamp, and a double-mixing apparatus at 277 K.[50, 51] For measurements of the heme-DNA complex systems, 5 μM heme and 10 μM DNA in 50 mM potassium phosphate buffer (pH 6.80) and 300 mM KCl were mixed with 15 mM H_2O_2. On the other hand, 5 μM HRP was mixed with 1 mM H_2O_2 in 50 mM potassium phosphate buffer, pH 6.80.

3. Results

Kinetics Measurements. The peroxidase activities of the heme(Fe^{3+})-6mer and heme(Fe^{3+})-6mer/A complexes were evaluated using Amplex Red as a substrate, and the initial slope (R_0) of the time evolution of 570-nm absorbance due to the oxidized product, 7-hydroxyphenoxazin-3-one (Resorufin), was used as an index for the activity, as reported previously[32, 45] (Figure 2A). The peroxidase activity of HRP, as a reference, was similarly measured and evaluated. The R_0s of the complexes and HRP in the presence of various H_2O_2 concentrations ([H_2O_2]) at 298 K were determined using the Michaelis-Menten equation to yield Michaelis constants for H_2O_2 ($K_m(H_2O_2)$) and catalytic rate constants (k_{cat}) (Figure 2B and C, and Table 1). The $K_m(H_2O_2)$ and k_{cat} of the heme(Fe^{3+})-6mer complex were larger and smaller by factors of ~3 and ~1/3 relative to the corresponding parameters of the heme(Fe^{3+})-6mer/A complex, respectively. As compared with the values obtained for HRP, the $K_m(H_2O_2)$s and k_{cat}s of the complexes were significantly larger and smaller, respectively (Table 1).

ESR Spectra. ESR spectra of the heme(Fe^{3+})-6mer and heme(Fe^{3+})-6mer/A complexes were measured in 50 mM potassium phosphate buffer (pH 6.80) at 5 K (Figure 3A and B) In the spectra, axial signals at $g_\perp$ = 5.95 and $g_\parallel$ = 2.00 were observed, and these signals were markedly similar to those reported for the acidic met-forms of native Mb and its variants.[52] In addition, a rhombic high-spin type signal was also observed at g = 6.33 in the spectrum of the heme(Fe^{3+})-6mer complex (Figure 3A), whereas such a signal was not observed in the spectrum of the heme(Fe^{3+})-6mer/A complex (Figure 3B). Furthermore, unidentified broad peaks were observed near g = 2 in the spectra of the heme(Fe^{3+})-6mer and heme(Fe^{3+})-6mer/A complexes (Figure 3A and B).

The spectra of samples prepared by freesing mixtures of the complex ([heme(Fe^{3+})-6mer complex] or [heme(Fe^{3+})-6mer/A complex] = 0.1 mM) and [H_2O_2] = 15 mM in phosphate buffer solutions, pH 6.80 (the interval between mixing and freezing being ~3 s), exhibited convex peaks at g ~ 2 (Figures 3A' and B'), which were similar to the spectral characteristics of Compound I[46,47, 53-57], i.e., an iron(IV)oxo porphyrin π-cation radical complex, as observed for the HRP sample similarly prepared from a solution mixture of [HRP] = 0.1 mM and [H_2O_2] = 0.2 mM (see Figure S1 in the Supporting Information). In addition, a signal at g ~ 6, derived from an unreacted ferric high-spin species, and one at g ~ 4.3 due to degraded heme[57] were observed, as seen in Figure 3A' and B', and the rhombic high-spin type signal at g = 6.33 was observed as a shoulder of a peak at g = 5.94 in the spectrum of the heme(Fe^{3+})-6mer complex (Figure 3A'). On the other hand, the convex peak at g ~ 2 due

Table 1. Steady state kinetics parameters for H_2O_2 oxidation of Amplex Red catalyzed by the heme(Fe^{3+})-6mer and heme(Fe^{3+})-6mer/A complexes, and HRP in 50 mM potassium phosphate buffer, pH 6.80, 300 mM KCl, at 298 K.

	K_m[a] (mM)	K_{cat}[a] (s^{-1})	K_{cat}/K_m (mM^{-1} s^{-1})
Heme(Fe^{3+})-6mer complex	163 ± 2	18 ± 1	0.11
Heme(Fe^{3+})-6mer/A complex	60 ± 7	51 ± 2	0.85
HRP	0.04 ± 0.01	1100 ± 40	28000

[a] Obtained by fitting of the plots shown in Figure 2B and C to the Michaelis-Menten equation.

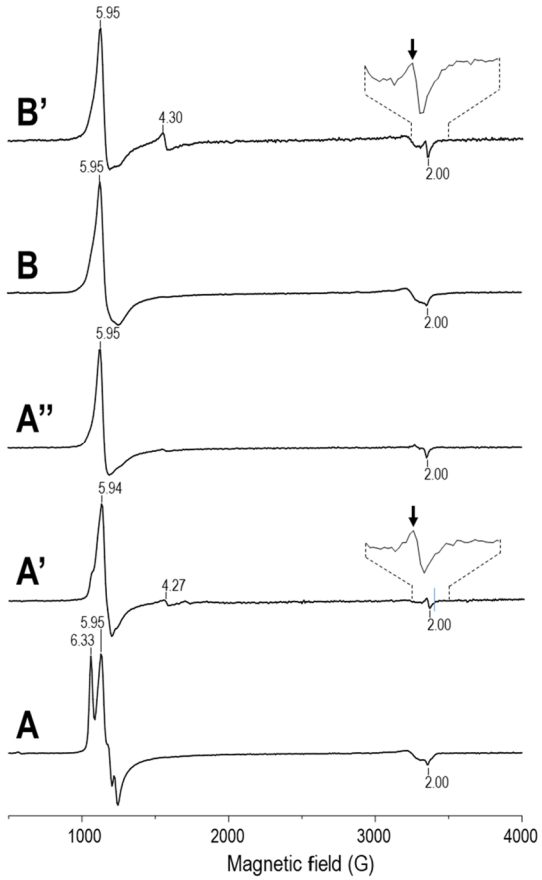

Figure 3. ESR spectra of the heme(Fe^{3+})-6mer complex (A) and heme(Fe^{3+})-6mer/A one (B) at 5K. Spectra recorded for samples prepared in 50 mM potassium phosphate buffer, pH 6.80, by addition of a 150-fold stoichiometric excess of H_2O_2 to the heme(Fe^{3+})-6mer complex in the absence (A') and presence of the substrate, Amplex Red (A''), and that recorded for the heme(Fe^{3+})-6mer/A complex after addition of a 150-fold stoichiometric excess of H_2O_2 to the heme(Fe^{3+})-6mer/A complex (B'). In (A') and (B'), the Y-gains of signals near g = 2 are expanded by a factor of ~2.5 and convex peaks at g = ~2 due to Compound I are indicated by downward pointing arrows.

to Compound I was not detected even though H_2O_2 was added to the heme(Fe^{3+})-6mer complex in the presence of the substrate, Amplex Red, and only signals due to a ferric high-spin species and degraded heme were observed (Figure 3A'').

Stopped-flow Experiments. A stopped-flow apparatus[50,51] was used to detect short-lived intermediates in the reaction of the heme(Fe^{3+})-6mer or heme(Fe^{3+})-6mer/A complex with H_2O_2 at pH 6.8 and 277 K. The absorption maximum of the Soret band of the heme(Fe^{3+})-6mer/A complex, i.e., 406 nm, was red-shifted by 3 nm relative to that of the heme(Fe^{3+})-6mer one, i.e., 403 nm (Figure 4A), indicating that the heme environment in the heme(Fe^{3+})-6mer complex is affected by the addition of the extra A at the 3'-terminal of the DNA, i.e., A7. Upon addition of a large excess of H_2O_2 to the aqueous solution containing the heme(Fe^{3+})-6mer complex, a gradual decrease in the Soret band was observed (Figure 4B). Since photodegradation of the complex during stopped-flow measurements is essentially negligible (Figure S2A and B in the Supporting Information), the decrease in the Soret band could be due to the formation of Compound I, although UV-Vis spectral signatures of Compound I[48, 49] were not apparent (see below).

In contrast, the addition of a large excess of H_2O_2 to the heme(Fe^{3+})-6mer/A complex resulted in an apparent biphasic change in the Soret band, such that the Soret band initially exhibited a rapid decrease and then a gradual one (Figure 4C). As shown in Figure 4D, the spectrum of the heme(Fe^{3+})-6mer/A complex was markedly altered by the addition of H_2O_2, and a drastic decrease in the Soret band and an increase at ~350 nm in the spectrum recorded after the H_2O_2 addition are similar to the UV-Vis spectral signatures of Compound I[48, 49] (see also Figure S2C and D in the Supporting Information).

4. Discussion

Peroxidase Activity. Analysis of the [H_2O_2]-dependent R_0 change observed for the heme(Fe^{3+})-6mer and heme(Fe^{3+})-6mer/A complexes using the Michaelis-Menten equation yielded K_m(H_2O_2)s and k_{cat}s of the complexes that were significantly larger and smaller than the corresponding ones of HRP, respectively (Table 1). The difference in the K_m(H_2O_2) between the complex and HRP could be to some extent due to their distinct heme coordination structures. We found, through NMR characterization of a carbon monoxide (CO) adduct of the heme(Fe^{2+})-6mer complex, that a water molecule sandwiched between the heme and G6 G-quartet planes is coordinated to the Fe atom as the other axial ligand (axial H_2O_{int}), *trans* to axial CO, and is hydrogen-bonded to the carbonyl oxygen atoms of G6 bases (Figure 1D).[31] Upon the oxidation of the heme Fe center in the CO adduct of the heme(Fe^{2+})-6mer complex to heme(Fe^{3+}), the Fe-bound CO in the complex is thought to be replaced by H_2O (axial H_2O_{ext}), while axial H_2O_{int} is retained, and, as a result, a *bis*-H_2O-coordinated heme(Fe^{3+}), i.e., heme(Fe^{3+}) possessing H_2O_{int} and H_2O_{ext} as axial ligands, in the heme(Fe^{3+})-DNA complex is formed under low pH conditions.[32] Therefore binding of H_2O_2 to the heme Fe^{3+} center of the complex proceeds through a ligand replacement reaction, as opposed to the binding of H_2O_2 to a penta-coordinated heme(Fe^{3+}) of resting state HRP[44, 58, 59] through a simple second-order reaction. Hence the H_2O_2 binding affinity of the heme(Fe^{3+})-6mer complex is intrinsically lower compared with that of resting state HRP, as reflected on the finding that the K_m(H_2O_2) of the complex is considerably larger than that of HRP. The peroxidase activities of the complexes could be interpreted on the basis of the push-pull mechanism,[32, 45] as in the case of the catalytic cycle of HRP (Scheme 1A). We found that the donor strength of the axial H_2O_{int} ligand in the heme(Fe^{3+})-6mer complex is markedly weaker than that of the proximal His in Mb.[32] Furthermore, the imidazolate character of the axial His170 in HRP was shown to be enhanced through the formation of a strong hydrogen bond with Asp247 (Scheme 1B), and hence the donor strength of the His170 in HRP is even stronger than that of the proximal His in Mb.[43, 58, 60] Therefore, the push mechanism due to the axial His170, together with the pull one due to both His42 and Arg38, in HRP contributes significantly to the increase in the activity (Scheme 1B). Consequently, the low peroxidase activity of the heme(Fe^{3+})-6mer complex is due to the weak donating ability of the axial H_2O_{int}, in addition to the absence of functional groups capable of furnishing the pull mechanism in the complex. Hence, the ~3-fold increase in the k_{cat} on the addition of an extra A at the 3'-terminal of the sequence indicated that the 3'-terminal A of the heme(Fe^{3+})-6mer/A complex acts as a general acid-base catalyst that promotes Compound I formation through its pull mechanism (Scheme 2).

ESR Detection of Compound I. In the ESR spectrum of the heme(Fe^{3+})-6mer complex at 5 K, an axial high-spin signal with $g_\perp$ = 5.95 and $g_\parallel$ = 2.00, and a rhombic high-spin-type signal

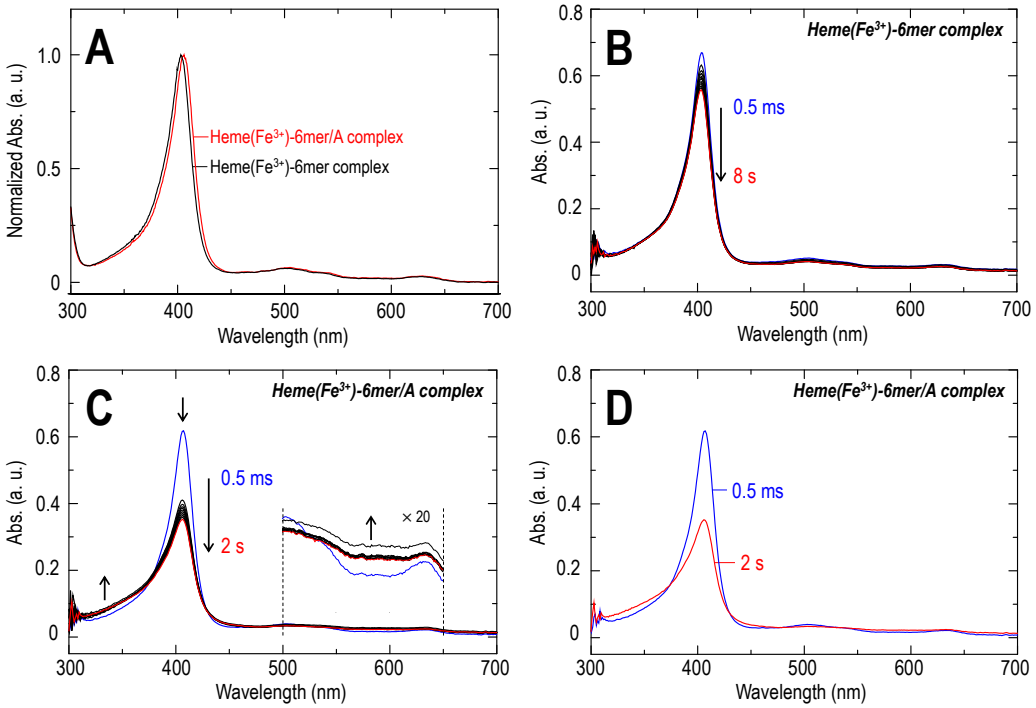

Figure 4. UV-Vis absorption spectra of the heme(Fe^{3+})-6mer (black) and heme(Fe^{3+})-6mer/A complexes (red) in 300 mM KCl, 50 mM potassium phosphate buffer, pH 6.80, at 298 K (A), and absorption spectral changes in the course of the reactions, for time spans of ~0.5 ms to 8 s, of the heme(Fe^{3+})-6mer complex with a 1500-fold stoichiometric excess of H_2O_2 in 50 mM potassium phosphate buffer, pH 6.80, and 300 mM KCl at 277 K, monitored with a time interval of 40 ms with a stopped-flow spectrometer (B). In (B), the spectra recorded with an interval of 800 ms are shown. Absorption spectral changes in the course of the reactions, for time spans of ~0.5 ms to 2 s, of the heme(Fe^{3+})-6mer/A complex with a 1500-fold stoichiometric excess of H_2O_2 in 50 mM potassium phosphate buffer, pH 6.80, and 300 mM KCl at 277 K, monitored with a time interval of 40 ms with a stopped-flow spectrometer (C). In (C), the spectra recorded with an interval of 200 ms are shown, and the Y-gains of the regions 500 – 650 nm are expanded by a factor of ~20. The spectra of the heme(Fe^{3+})-6mer/A complex, recorded at ~0.5 ms (blue) and 2 s (red) after the addition of H_2O_2, extracted from (C) are compared (D).

with $g = 6.33$ were observed (Figure 3A). The spectrum of the complex at 298 K previously reported[26] was axial, and hence a species with a rhombic symmetry of the d electron system was not detected. Therefore, the axial high-spin signals observed in the spectra at 5 K and 298 K could be due to *bis*-H_2O-coordinated heme(Fe^{3+}) in the complex, with axial symmetry of the d electron system. In addition, the rhombic high-spin species detected in the spectrum of the complex at 5 K might be due to the presence of two (or more) orientations of the axial H_2O_{ext}, with respect to the heme(Fe^{3+}), which possibly influences the axial symmetry of the high-spin ferric center. In contrast to the case of the heme(Fe^{3+})-6mer complex, the spectrum of the heme(Fe^{3+})-6mer/A complex at 5 K did not exhibit a rhombic high-spin-type signal, and hence the orientation of the axial H_2O_{ext}, with respect to the heme(Fe^{3+}), might be fixed through its interaction with the 3'-terminal A, i.e., A7, in the complex. Furthermore, the broad peaks near $g = 2$ in the ESR spectra of the complexes (Figures 3A and B) are likely to be due to the presence of unidentified minor species in the samples, and similar broad ones near $g = 2$ could also be detected in the spectrum of a complex between heme and a G-quadruplex heme-binding DNA aptamer.[3]

An asymmetric signal, with a line width of ~15 G, at $g = 1.995$ has been reported to be an ESR spectral signature of Compound I.[46] The broadening of the Compound I signal is due to short electron spin relaxation times through spin-exchange interaction between the porphyrin π-cation radical ($S = 1/2$) and the iron center ($S = 1$).[61, 62] The newly-emerged convex peaks at $g \sim 2$ in the spectra of the frozen samples of mixtures of the complexes and H_2O_2 exhibited such ESR characteristics of Compound I (Figure 3 A' and B'), supporting Compound I formation in the heme(Fe^{3+})-6mer and heme(Fe^{3+})-6mer/A complex systems. Furthermore, Compound I was not formed even though H_2O_2 was added to the heme(Fe^{3+})-6mer complex in the presence of Amplex Red (Figure 3A''), demonstrating that Compound I was rapidly consumed through oxidation of the substrate. Thus, on the basis of these ESR spectra, the formation of Compound I as an intermediate in the peroxidase catalytic cycles of the complexes was confirmed.

Stopped-flow Detection of Compound I. Since Compound I exhibits a characteristic absorption spectrum,[48, 49] the stopped-flow technique has frequently been used to detect this short-lived intermediate in the peroxidase catalytic cycle. The absorption spectral signatures of Compound I were clearly observed in the spectrum of the heme(Fe^{3+})-6mer/A complex (Figure 4C), although it was not apparent in the spectra of the heme(Fe^{3+})-6mer one (Figure 4B). In the spectrum of Compound I, an increase at ~350 nm, and small absorption maxima at ~580 and ~650 nm are observed, and these features have been recognized as its UV-Vis spectral signatures[48, 49]. Besides these spectral signatures of Compound I, a decrease in the Soret band is likely to be most prominent among the spectral

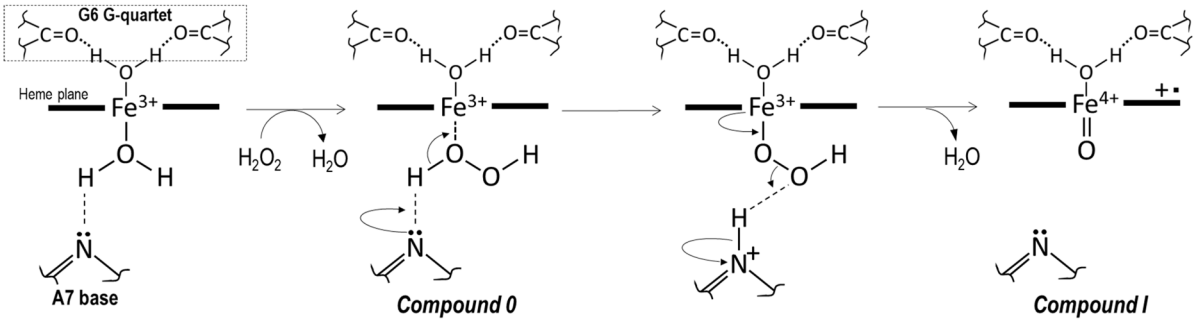

Scheme 2. "Pull mechanism" possibly provided by A7 base of the heme(Fe^{3+})-6mer/A complex, which facilitates heterolytic O-O bond cleavage of Fe-bound hydrogen peroxide (H_2O_2). A similar mechanism has been proposed previously.[22-24] The axial H_2O molecule is sandwiched between the heme and G-quartet planes[31, 32] and the hydrogen bond between Fe-bound H_2O and the nearby A7 base[45] is added to the proposed mechanism as a dotted line.

changes observed upon the conversion of a ferric high-spin heme complex to Compound I (see Figure S2D in the Supporting Information). Hence, the rapid decrease in the Soret band observed in Figure 4B might be considered as an indicator of the formation of Compound I, although bleaching of the complex by H_2O_2 cannot be ruled out. The observation of an ESR spectral signature of Compound I, i.e., a convex peak at $g \sim 2$, in the spectrum of a sample prepared by freezing a mixture of the complex and H_2O_2 within ~3 s (Figure 3A') supported this interpretation. As far as the sensitivities of the techniques for detecting Compound I are concerned, the ESR technique, which relies on the observation of its characteristic signal at $g \sim 2$, would be advantageous over the UV-Vis one, which is possibly hampered by spectral overlap between a ferric high-spin heme complex and Compound I, particularly in cases where only a trace amount of Compound I is formed in samples, such as the case shown in Figure 4B.

In contrast, as manifested in the enhanced peroxidase activity of the heme(Fe^{3+})-6mer/A complex relative to that of the heme(Fe^{3+})-6mer one (Table 1), the "pull" mechanism provided by the 3'-terminal A accelerated the Compound I formation so that an appreciable amount of Compound I was rapidly formed in the heme(Fe^{3+})-6mer/A complex system upon the addition of H_2O_2 (Figure 4C). As described above, since the conversion of a ferric high-spin heme complex to Compound I results in a considerable decrease in the Soret band (Figure S2D in the Supporting Information), the time scale of the decrease in the Soret band of the system is thought to be accelerated with increasing rate of Compound I formation. Consequently, the rapid decrease in the Soret band of the heme(Fe^{3+})-6mer/A complex system, relative to that of the heme(Fe^{3+})-6mer complex counterpart, also supported enhancement of the rate of Compound I formation through the "pull" mechanism provided by the 3'-terminal A, which ensured the formation of Compound I enough to observe its characteristic absorption spectrum (Figure 3B).

Peroxidase Catalytic Cycle of Heme-DNAzymes. The peroxidase activity of heme(Fe^{3+}) is dramatically enhanced when it is bound to the G-quartet.[1-8, 32, 45] The enhancement of the catalytic activity of heme(Fe^{3+}) through its interaction with nucleic acids is likely to be relevant to primordial chemistry as well as to current biology. In addition, elucidation of the structure-function relationship of heme-DNAzymes not only leads to the discovery of a novel mechanism for control of the heme(Fe^{3+}) reactivity in the scaffold of nucleic acids, but also paves a way to the creation of novel heme-DNAzymes.

Although the molecular mechanism responsible for the enhancement of the intrinsic peroxidase activity of heme(Fe^{3+}) through interaction with DNA has yet to be fully elucidated, it has been shown that binding to heme(Fe^{3+}) to a folded DNA is not sufficient to activate heme(Fe^{3+}).[2] We found that, in the complex, a water molecule (H_2O), sandwiched between the heme and G-quartet planes, is coordinated to the Fe center as an axial ligand.[31, 32] Theoretical study indicated that the polarization of the H_2O molecule is considerably greater than that of an ordinary one,[31] and hence the axial H_2O in the complex is possibly capable of being an electron-donating ligand which increases the Lewis basicity of the heme Fe atom to activate Fe-bound H_2O_2 for the reaction.

The peroxidase activity of heme-DNAzymes has been assumed to be elicited through a reaction mechanism essentially identical to the HRP peroxidation cycle.[12, 24] The proposed mechanism for heme-DNAzymes[12, 24] has been supported indirectly by the findings that demonstrated that the "push-pull" mechanism is operative in the heme-DNAzyme peroxidation cycle.[23, 32, 45] In this study, using ESR spectroscopy and stopped-flow measurements, we could detect Compound I formed in the heme(Fe^{3+})-6mer and heme(Fe^{3+})-6mer/A complex systems, providing direct evidence of the catalytic mechanism of the complexes. Hence the mechanism for the heme-DNAzyme peroxidation cycle was proved to be identical to that for the HRP one. This finding will allow us to design and enhance the catalytic activity of heme-DNAzymes with reference to the HRP peroxidation mechanism.

5. Concluding Remarks

We could detect a high valent iron(IV)oxo porphyrin π-cation radical species known as Compound I formed in the peroxidase catalytic cycle of heme-DNAzymes composed of heme, heme(Fe^{3+}), and all parallel-stranded tetrameric G-quadruplex DNAs related to a single repeat sequence of the human telomere, i.e., d(TTAGGG) and d(TTAGGGA). This finding confirmed that the peroxidase activity of heme-DNAzymes is realized through Compound I, as in the case of heme enzymes such as HRP. Since functional groups involved in the peroxidation cycle of the heme-DNAzymes are different from those of HRP, elucidation of the structure-function relationship in the heme-DNAzymes will lead to discovery of a novel mechanism for control of the heme(Fe^{3+}) reactivity, which will contribute to exploration of the biological versatility of heme as a prosthetic group of nucleic acid catalysts. Furthermore, since heme is believed to be an ancient compound,[63] the results presented here provide a new insight

into the concept of a primordial "RNA world" [64] by demonstrating the redox-catalyzing ability of heme in the scaffold of nucleic acids, which will expand the repertories of nucleic acid catalysts.

Acknowledgement

This work was financially supported by JSPS KAKENHI (No. 16KT0048 to Y.Y. and 17H03027 to T.K.), and the Bilateral Open Partnership Joint Research Project (No. BBD29011 to Y.Y.).

References

1. P. Travascio, Y. Li, D. Sen, *Chem. Biol.* **1998**, *5*, 505.
2. P. Travascio, A. J. Bennet, D. Y. Wang, D. Sen, *Chem. Biol.* **1999**, *6*, 779.
3. P. Travascio, P. K. Witting, A. G. Mauk, D. Sen, *J. Am. Chem. Soc.* **2001**, *123*, 1337.
4. P. Travascio, D. Sen, A. J. Bennet, *Can. J. Chem.* **2006**, *84*, 613.
5. L. C.-H. Poon, S. P. Methot, W. Morabi-Pazooki, F. Pio, A. J. Bennet, D.Sen, *J. Am. Chem. Soc.* **2011**, *133*, 1877.
6. Y. Li, D. Sen, *Chem. Biol.* **1998**, *5*, 1.
7. D. Sen, C. R. Geyer, *Curr. Opin. Chem. Biol.* **1998**, *2*, 680.
8. D. Sen, L. C. Poon, *Crit. Rev. Biochem. Mol. Biol.* **2011**, *46*, 478.
9. I. Willner, B. Shlyahovsky, M. Zayats, B. Willner, *Chem. Soc. Rev.* **2008**, *37*, 1153.
10. J. Kosman, B. Juskowiak, *Anal. Chim. Acta* **2011**, *707*, 7.
11. R. Freeman, E. Sharon, C. Teller, A. Henning, Y. Tzfati, I. Willner, *ChemBioChem* **2010**, *11*, 2362.
12. L. Stefan, H. J. Xu, C. P. Gros, F. Denat, D. Monchaud, *Chem. - A Eur. J.* **2011**, *17*, 10857.
13. D. Kong, J. Xu, H. Shen, *Anal. Chem.* **2010**, *82*, 6148.
14. X. Yang, C. Fang, H. Mei, T. Chang, Z. Cao, D. Shangguan, *Chem. - A Eur. J.* **2011**, *17*, 14475.
15. E. Golub, R. Freeman, I. Willner, *Angew. Chemie - Int. Ed.* **2011**, *50*, 11710.
16. E. Golub, R. Freeman, I. Willner, *Anal. Chem.* **2013**, *85*, 12126.
17. E. Sharon, E. Golub, A. Niazov-Elkan, D. Balogh, I. Willner, *Anal. Chem.* **2014**, *86*, 3153.
18. X. Liu, A. Niazov-Elkan, F, Wang, I. Willner, *Nano Lett.* **2013**, *13*, 219.
19. E. Golub, H. B. Albada, W. C. Liao, Y. Biniuri, I. Willner, *J. Am. Chem. Soc.* **2016**, *138*, 164.
20. Z. Zhou, X. Liu, L. Yue, I. Willner, *ACS Nano* **2018**, *12*, 10725.
21. Y. Sun, X. Wang, H. Xu, C. Ding, Y. Lin, C. Luo, Q. Wei, *Anal. Chim. Acta* **2018**, *1043*, 132.
22. L. Stefan, F. Denat, D. Monchaud, *Nucleic Acids Res.* **2012**, *40*, 8759.
23. W. Li, Y. Li, Z. Liu, B. Lin, H. Yi, F. Xu, Z. Nie, S. Yao, *Nucleic Acids Res.* **2016**, *44*, 7373.
24. J. Chen, Y. Zhang, M. Cheng, Y. Guo, J. Šponer, D. Monchaud, J.-L. Mergny, H. Ju, J. Zhou, *ACS Catal.* **2018**, *8*, 1352.
25. D. Sen, W. Gilbert, *Nature* **1998**, *334*, 364.
26. T. Mikuma, T. Ohyama, N. Terui, Y. Yamamoto, H. Hori, *Chem. Commun.* **2003**, 1708.
27. T. Ohyama, Y. Kato, H. Mita, Y. Yamamoto, Y. *Chem. Lett.* **2006**, *35*, 126.
28. K. Saito, H. Tai, M. Fukaya, T. Shibata, R. Nishimura, S. Neya, Y. Yamamoto, *J. Biol. Inorg. Chem.* **2012**, *17*, 437.
29. K. Saito, H. Tai, H. Hemmi, N. Kobayashi, Y. Yamamoto, *Inorg. Chem.* **2012**, *51*, 8168.
30. Y. Suzuki, H. Tai, K. Saito, T. Shibata, M. Kinoshita, A. Suzuki, Y. Yamamoto, *J. Porphyr. Phthalocyanines* **2014**, *18*, 741.
31. Y. Yamamoto, M. Kinoshita, Y. Katahira, H. Shimizu, Y. Di, T. Shibata, H. Tai, A. Suzuki, S. Neya, *Biochemistry* **2015**, *54*, 7168.
32. R. Shinomiya, Y. Katahira, H. Araki, T. Shibata, A. Momotake, S. Yanagisawa, T. Ogura, A. Suzuki, S. Neya, Y. Yamamoto, *Biochemistry* **2018**, *57*, 5930.
33. M. Sono, M. P. Roach, E. D. Coulter, J. H. Dawson, *Chem. Rev.* **1996**, *96*, 2841.
34. J. H. Dawson, M. Sono, *Chem. Rev.* **1987**, *87*, 1255.
35. T. L. Poulos, B. C. Finzel, A. J. Howard, *J. Mol. Biol.* **1987**, *195*, 687.
36. T. L. Poulos, *Adv. Inorg. Biochem.* **1988**, *7*, 1.
37. T. L. Poulos, *Curr. Opin. Struct. Biol.* **1995**, *5*, 767.
38. J. H. Dawson, *Science* **1988**, *240*, 433.
39. J. H. Dawson, R. H. Holm, J. R. Trudell, G. Barth, R. E. Linder, E. Bunnenberg, C. Djerassi, S. C. Tang, *J. Am. Chem. Soc.* **1976**, *98*, 3707.
40. N. C. Gerber, S. G. Sligar, *J. Am. Chem. Soc.* **1992**, *114*, 8742.
41. N. C. Gerber, S. G. Sligar, *J. Biol. Chem.* **1994**, *269*, 4260.
42. Y. Kimata, H. Shimada, T. Hirose, Y. Ishimura, Y. *Biochem. Biophys. Res. Commun.* **1995**, *208*, 96.
43. J. N. Rodríguez-López, D. J. Lowe, J. Hernández-Ruiz, A. N. Hiner, F. García-Cánovas, R. N. Thorneley, *J. Am. Chem. Soc.* **2001**, *123*, 11838.
44. M. Gajhede, D. J. Schuller, A. Henriksen, A. T. Smith, T. J. Poulos, *Nat. Struct. Biol.* **1997**, *4*, 1032.
45. Y. Yamamoto, H. Araki, R. Shinomiya, Y. Hayasaka, Y. Nakayama, K. Ochi, T. Shibata, A. Momotake, T. Ohyama, M. Hagihara, H. Hemmi, *Biochemistry* **2018**, *57*, 5938.
46. R. Aasa, T. Vänngård, H. B. Dunford, *Biochim. Biophys. Acta* **1975**, *391*, 259.
47. M. Tanaka, K. Matsuura, S. Yoshioka, S. Takahashi, K. Ishimori, H. Hori, I. Morishima, *Biophys. J.* **2003**, *84*, 1998.
48. W. Hewson, L. P. Hager, *J. Biol. Chem.* **1979**, *254*, 3182.
49. J. Rittle, M. T. Green, *Science* **2010**, *330*, 933.
50. H. Mitome, T. Ishizuka, H. Kotani, Y. Shiota, K. Yoshizawa, T. Kojima, *J. Am. Chem. Soc.* **2016**, *138*, 9508.
51. H. Kotani, S. Kaida, T. Ishizuka, K. Mieda, M. Sakaguchi, T. Ogura, Y. Shiota, K. Yoshizawa, T. Kojima, *Inorg. Chem.* **2018**, *57*, 13929.
52. M. Ikeda-saito, H. Hori, L. A. Andersson, R. C. Prince, I. J. Pickering, G. N. George, C. R. Sanders. R. S. Lutz, E. J. Mckelvey, R. Mattera, *J. Biol. Chem.* **1992**, *267*, 22843.
53. W. E. Blumberg, J. Peisach, B. A. Wittenberg, J. B. Wittenberg, *J. Biol. Chem.* **1968**, *243*, 1854.
54. M. J. Benecky, J. E. Frew, N. Scowen, P. Jones, B. M. Hoffman, *Biochemistry* **1993**, *32*, 11929.
55. W. R. Patterson, T. L. Poulos, D. B. Goodin, *Biochemistry* **1995**, *34*, 4342.
56. H. Fujii, T. Yoshimura, H. Kamada, *Inorg. Chem.* **1996**, *35*, 2373.
57. M. Tanaka, K. Ishimori, M. Mukai, T. Kitagawa, I. Morishima, *Biochemistry* **1997**, *36*, 9889.
58. R. Evangelista-Kirkup, G. Smulevich, T. G. Spiro, *Biochemistry* **1986**, *25*, 4420.
59. G. N. La Mar, J. S. de Ropp, K. M. Smith, K. C. Langry, *J. Biol. Chem.* **1980**, *255*, 6646.
60. E. Derat, S. Shaik, *J. Phys. Chem. B* **2006**, *110*, 10526.
61. R. Rutter, L. P. Hager, H. Dhonau, M. Hendrich, M. Valentine, P. Debrunner, *Biochemistry* **1984**, *23*, 6809.
62. C. E. Schulz, P. W. Devaney, H. Winkler, P. G. Debrunner, N. Doan, R. Chiang, R. Rutter, L. P. Hager, *FEBS Lett.*

1979, *103*, 102.
63. M. Yarus, *Annu. Rev. Genet.* **2002**, *36*, 125.
64. W. Gilbert, *Nature* **1986**, *319*, 618.